Cell Transplantation, Vol. 22, pp. 369–379, 2013

0963-6897/13 $90.00 + .00
DOI: http://dx.doi.org/10.3727/096368911X582769
E-ISSN 1555-3892
www.cognizantcommunication.com

The Immunosuppressive Effect of Mesenchymal Stromal Cells on B Lymphocytes Is Mediated by Membrane Vesicles

Manuela Budoni,*[1] Alessandra Fierabracci,*[1] Rosa Luciano,*
Stefania Petrini,* Vincenzo Di Ciommo,† and Maurizio Muraca*

*Research Laboratories, Children's Hospital "Bambino Gesù" Research Institute, Rome, Italy
†Service of Epidemiology and Biostatistics, Children's Hospital "Bambino Gesù" Research Institute, Rome, Italy

The immunomodulatory properties of mesenchymal stromal cells are the subject of increasing interest and of widening clinical applications, but the reproducibility of their effects is controversial and the underlying mechanisms have not been fully clarified. We investigated the transfer of membrane vesicles, a recently recognized pathway of intercellular communication, as possible mediator of the interaction between mesenchymal stromal cells and B lymphocytes. Mesenchymal stromal cells exhibited a strong dose-dependent inhibition of B-cell proliferation and differentiation in a CpG-stimulated peripheral blood mononuclear cell coculture system. We observed that these effects could be fully reproduced by membrane vesicles isolated from mesenchymal stromal cell culture supernatants in a dose-dependent fashion. Next, we evaluated the localization of fluorescently labeled membrane vesicles within specific cell subtypes both by flow cytometry and by confocal microscopy analysis. Membrane vesicles were found to be associated with stimulated B lymphocytes, but not with other cell phenotypes (T lymphocytes, dendritic cells, natural killer cells), in peripheral blood mononuclear cell culture. These results suggest that membrane vesicles derived from mesenchymal stromal cells are the conveyors of the immunosuppressive effect on B lymphocytes. These particles should be further evaluated as immunosuppressive agents in place of the parent cells, with possible advantages in term of standardization, safety, and feasibility.

Key words: Mesenchymal stromal cells (MSCs); Membrane vesicles (MVs); Immunomodulation; B lymphocytes; Proliferation; Differentiation

INTRODUCTION

Mesenchymal stromal cells (MSCs) have immunomodulatory properties demonstrated in vitro, in animal studies, and in clinical applications such as the treatment of severe graft versus host disease (GVHD) (4,16,31). However, the underlying mechanisms have not been fully clarified (19,21). In particular, while the suppressive effect of MSCs on activated T-cells has been extensively investigated and found to involve multiple factors (2,17,24), both the effect of MSCs on B-cells and the involved mechanisms are more controversial (8,10,22,26,28). Recently, it was demonstrated that several interactions between immune cells are mediated by secreted membrane vesicles (MVs) (27). Various types of secreted MVs have been described, ranging from 50 to 1,000 nm in diameter and exhibiting distinct structural and biochemical properties according to their intracellular site of origin, features probably also affecting their function (5). An increasing body of evidence indicates that they play a pivotal role in cell-to-cell communication (7); in particular, MVs can play a role in intercellular signaling by exchanging mRNA, microRNA, and proteins among cells within a defined microenvironment (29). The aim of this study was to verify the immunomodulatory properties of MVs derived by MSCs (MSC-MVs) on B-cell function. Here, we show that the immunosuppressive effect of MSCs on B-cells can be reproduced in a dose-dependent fashion by MSC-MVs secreted in the medium by cultured cells.

MATERIALS AND METHODS

MSC Culture and Expansion

Commercially available bone marrow human MSCs (Lonza, Basel, Switzerland) were plated in 75-cm^2 polystyrene vented tissue culture flasks (Becton Dickinson, BD, Franklin Lakes, NJ, USA) at a density of 4×10^3 cells/cm^2 in a volume of 10 ml of MesenCult basal medium

Received August 2, 2011; final acceptance March 12 ,2012. Online prepub date: August 27, 2012.
[1]These authors provided equal contribution to this work.
Address correspondence to Prof. Maurizio Muraca, Research Laboratories, Children's Hospital "Bambino Gesù," Piazza Sant'Onofrio, 4, 00165 Rome, Italy. Tel: +39 06 6859 2210; Fax +39 06 6859 2014; E-mail: maurizio.muraca@opbg.net

(StemCell Technologies, Vancouver, BC, Canada) supplemented with 20% fetal bovine serum (FBS; HyClone Laboratories), 100 U/ml penicillin, and 100 µg/ml streptomycin (Gibco, Grand Island, NY). In order to remove endogenous MVs, FBS was centrifuged overnight at 100,000×*g* before use. Cultures were incubated at 37°C in a humidified atmosphere containing 5% CO_2. Cells were subsequently maintained in the same medium and passaged at 80–90% confluence in a ratio 1:2 in trypsin/EDTA solution (Invitrogen, Life Technologies, Monza, Italy), with the medium changed once a week.

Peripheral Blood Mononuclear Cell Isolation

Blood samples from healthy donors were recruited at the Blood Transfusion Center of Children's Hospital Bambino Gesù, Rome. After obtaining informed consent, peripheral blood mononuclear cells (PBMCs) were separated by Ficoll-Hypaque (Histopaque, Sigma-Aldrich Chemical C, St. Louis, MO, USA) from 50 ml of sodium-heparinized venous blood samples, washed twice in Dulbecco's phosphate-buffered saline (D-PBS, EuroClone, Milan, Italy), and cryopreserved in liquid nitrogen until use. The protocol, involving the use of human material, was approved by the Ethical Committee of the Children's Hospital Bambino Gesù.

Coculture of PBMCs With MSCs

B-cell viability experiments were performed in a coculture system with MSCs plated in 96-multiwell culture plates (Corning-Costar, Celbio, Milan, Italy) at initial densities of 2.5×10^4, 1×10^4, or 5×10^3 cells/well in MesenCult basal medium supplemented with FBS (20%). For the immunomodulation experiments, MSCs were plated in 96-multiwell plates at a concentration of 5×10^3 cells/well and cultured in MesenCult basal medium supplemented with FBS (20%). On the following day, the medium was aspirated and replaced with PBMCs at 5×10^5 cells/well, corresponding to MSCs/PBMC ratios of 1:20, 1:50, and 1:100. In order to evaluate cell proliferation and differentiation, PBMCs had been prelabeled with 0.5 µM 5-chloromethylfluorescein diacetate (CMFDA, CellTracker; Molecular Probes) according to the manufacturer's guidelines and cocultured with MSCs in RPMI 1640 medium (BioWhittaker, Lona, Belgium) supplemented with 10% FBS. B-cell stimulation was achieved by incubation with 2.5 µg/ml human CpG oligodeoxynucleotides (5′-TCGTC GTTTTGTCGTTTTGTCGTT-3′)(HycultBiotechnology). After 1 week, the cocultures of PBMCs were rescued, washed in D-PBS, and analyzed by fluorescence-activated cell sorting (FACSCanto II, BD Biosciences).

Coculture of PBMCs With MSC-MVs

MSC-MVs were isolated with a modification of the procedure of Lamparski et al. (18). Cultures of MSCs at 90% confluence were used for the isolation of MVs. The medium from culture plates with 2×10^6 seeded MSCs was collected at day 5 of culture and centrifuged at 1,000×*g* for 20 min to remove the debris. Ten milliliters of clarified supernatant was concentrated by centrifugation for 20 min at 2,000×*g* in a sterile hydrated 30-kDa MWCO Amicon Ultra Centrifugal filter (Millipore, Bedford, MA) up to a volume of 15–20 µl. The MSC-conditioned concentrated medium was diluted in 10 ml of PBS in polyallomer tubes (Beckman Coulter, Milan, Italy), then ultracentrifuged at 100,000×*g* at 4°C for 1 h. At the end of the procedure, 2 ml was collected from the bottom of the tubes and concentrated by centrifuging for 20–30 min at 2,000×*g* in a sterile 30-kDa MWCO Amicon Ultra Centrifugal filter (Millipore) up to a volume of 15–20 µl. MVs were used either undiluted or diluted 1:3 or 1:6 in RPMI 1640 (BioWhittaker) and added to 5×10^5 CMFDA-labeled PBMCs 1 and 24 h after seeding. After 1 week in the presence of 2.5 µg/ml human CpG oligodeoxynucleotides added at the time of cell seeding, PBMCs were collected by centrifugation, washed, and analyzed by flow cytometry.

Detection of Apoptosis

For the detection of apoptosis, PBMCs cultured in medium alone, with CpG, or cocultured with MSC-MVs plus CpG were analyzed by Annexin V and 7-aminoactinomycin (7-AAD) staining. Briefly, after 4 and 7 days in culture, the cells were centrifuged at 300×*g* for 5 min and incubated with anti-CD19 [1:10, phycoerythrin-cyanine 7 (PE-Cy7) conjugated, Becton Dickinson, BD, Franklin Lakes, NJ, USA] for 20 min at 4°C in the dark. After washing with PBS, 5 µl of Annexin V [allophycocyanin (APC)-conjugated, BD] and 5 µl of vital dye 7-AAD [peridin-chlorophyll protein complex (PerCP)-conjugated, BD] were added in a final volume of 500 µl of Annexin V Binding Buffer 1× (BB1×) according to the manufacturer's guidelines. After 15 min of incubation in the dark at room temperature, the samples were transferred on fluorescence-activated cell sorting (FACS) tubes (BD) and acquired with a FACSCanto II (BD). Flow cytometry profiles were analyzed using FACSDiva software (BD). A minimum of 20,000 events were collected per data set.

Detection of Immunoglobulin Production

PBMCs were cocultured in 96-multiwell plates with or without incubation with MSC-MVs in RPMI 1640 (BioWhittaker) supplemented with 10% FBS (HyClone). After 1 week, the plates were centrifuged at 300×*g* for 5 min, and the supernatants were collected and tested by enzyme-linked immunosorbent assay (ELISA) in order to assess immunoglobulin production. The 96-multiwell ELISA plates (Corning) were coated with purified goat anti-human IgA or IgG or IgM diluted in PBS and incubated overnight at 4°C (IgA, 10 µg/ml;

IgG, 15 μg/ml; IgM, 2.5 μg/ml; Jackson ImmunoResearch Laboratories, West Grove, PA, USA). After three washes in PBS/Tween (0.1%), the supernatants from cell cultures were added to the plates (50 μl/well) and incubated at 37°C for 1 h in a humidified atmosphere. After washing, the plates were incubated for 1 h at 37°C with 50 μl of peroxidase-conjugated goat anti-human IgA (1:1,000), IgG (1:2,000), or IgM (1:1,000) diluted in PBS (Jackson ImmunoResearch Laboratories). *o*-Phenylenediamine tablets (Sigma-Aldrich), diluted in PBS according to the manufacturer's guidelines, were used as chromogenic substrate to develop the assay. The reaction was stopped after 30 min by adding 50 μl/well of SDS (10%). At the end of the procedure, the plates were read with a microplate spectrophotometer (Benchmark Plus) at 460 OD.

Flow Cytometry

At the end of the experiments, PBMCs were harvested from culture plates, centrifuged at 300×*g* for 5 min, and resuspended in PBS/FBS (2%). Single-cell suspensions were incubated in the dark for 20 min at 4°C with directly conjugated monoclonal antibodies (mAbs) directed against the following human surface molecules: CD19 (1:7, Cy5-conjugated), CD27 (1:7, PE-conjugated), CD38 (1:30, PE-Cy7-conjugated), IgM (1:100, Cy5-conjugated), CD86 (1:5, APC-conjugated), CD3 [1:7, fluorescein isothiocyanate-conjugated (FITC)], CD56 (1:7, FITC-conjugated), CD19 (1:20, APC-Cy7-conjugated). All antibodies were purchased from BD. After labeling, cells were washed twice in PBS/FBS (2%), and data were acquired with a FACSCanto II (BD). Flow cytometry profiles were analyzed using FACSDiva software (BD). A minimum of 20,000 events were collected per data set.

For selected experiments, the MVs derived from supernatant of 2×10^6 seeded MSCs grown at confluence were isolated with the procedure described above and added with 5 μl of Annexin V (APC-conjugated; BD) in conjunction with 5 μl of vital dye 7-AAD (PerCP-conjugated; BD) in a final volume of 500 μl of Annexin V Binding Buffer 1× (BB1×) according to the manufacturer's guidelines. After 15 min of incubation in the dark at room temperature, the MV samples were transferred to Troucount tubes (BD) containing calibration beads in order to gate the MVs by morphological parameters (forward scatter FSC-H; side scatter, SSC-H).

MSC-MV Cytokine Content

Pelletted MSC-MVs were mixed with Triton X-100 (1% final concentration), and the lysate was assayed with the FluoCytomix Multiple Analyte Detection kit (eBioscience, San Diego, CA, USA) according to the manufacturer's instructions. Assayed human cytokines included interferon (IFN)-γ, interleukin (IL)-1β, IL-2, IL-4, IL-5, IL-6, IL-8, IL-10, IL-12 p70, tumor necrosis factor (TNF)-α, and TNF-β. MSC-MVs were also maintained in culture medium at 37°C, and cytokine release was measured in medium after 2, 4, and 7 days.

Imaging Analysis of MSC-MV Association With PBMCs

MVs were isolated from the medium of 2×10^6 MSCs as described above and labeled with 2.5×10^{-6} M PKH26 (25) (Sigma, St. Louis, MO, USA) according to the manufacturer's instructions. The labeled MVs were gently added to the PBMC suspension (5×10^5 cells/well) in RPMI plus 10% FBS. After 1 h of incubation at 37°C in a humidified atmosphere with 5% CO_2, the cell population was washed in PBS and split in two aliquots for flow cytometry and for confocal microscopy analysis.

Immunofluorescence Analysis. PBMCs incubated with PKH26-labeled MVs were rinsed in PBS, fixed in 4% formaldehyde, blocked with PBS/FBS (5%) for 30 min, and single-labeled with the following monoclonal antibodies: anti-CD86 (1:10), anti-CD3 (1:10), and anti-CD19 (1:10), all conjugated to allophycocyanin (BD), as well as anti-CD56 antibody (1:30, FITC-conjugated; BD).

All antibodies were diluted in PBS/bovine serum albumin (BSA) (1%) and incubated for 1 h. Negative controls were performed using PBMC samples without incubation with MVs, as well as omitting the primary antibody in the staining procedure.

Nuclei were counterstained with 1 μg/ml Hoechst 33342 (Invitrogen, Molecular Probes, Eugene, OR, USA). After washing in PBS, the samples were mounted with ProLong antifade reagent (Invitrogen).

Confocal Laser Microscopy and Image Processing Analysis. Confocal imaging was performed on an Olympus Fluoview FV1000 confocal microscope equipped with FV10-ASW version 2.0 software, Multi Ar (458–488 and 515 nm), 2× He/Ne (543 and 633 nm), and 405-nm diode lasers, using a 60× (1.35 NA oil) objective. Optical single sections were acquired with a scanning mode format of 1,024×1,024 pixels, with a 207 nm/pixel size, sampling speed of 40 μs/pixel, and 12 bits/pixel images. Fluorochrome unmixing was performed by acquisition of automated sequential collection of multichannel images in order to reduce spectral crosstalk between channels. The pinhole aperture was 1 Airy unit.

Z-reconstruction of serial single optical sections was performed with a scanning mode of 1,024×1,024 pixels with an electronic zoom at 2, corresponding to 103 nm/pixel, sampling speed of 20 μs/pixel, and Z stack of 0.40 μs/slice. Images were processed using Photoshop software version 9.0 (Adobe Systems Inc., San Jose, CA, USA).

Statistical Analysis

Each experiment was run in duplicate, and the mean of the two results was calculated. Data were analyzed in terms of medians and minimum and maximum values. A

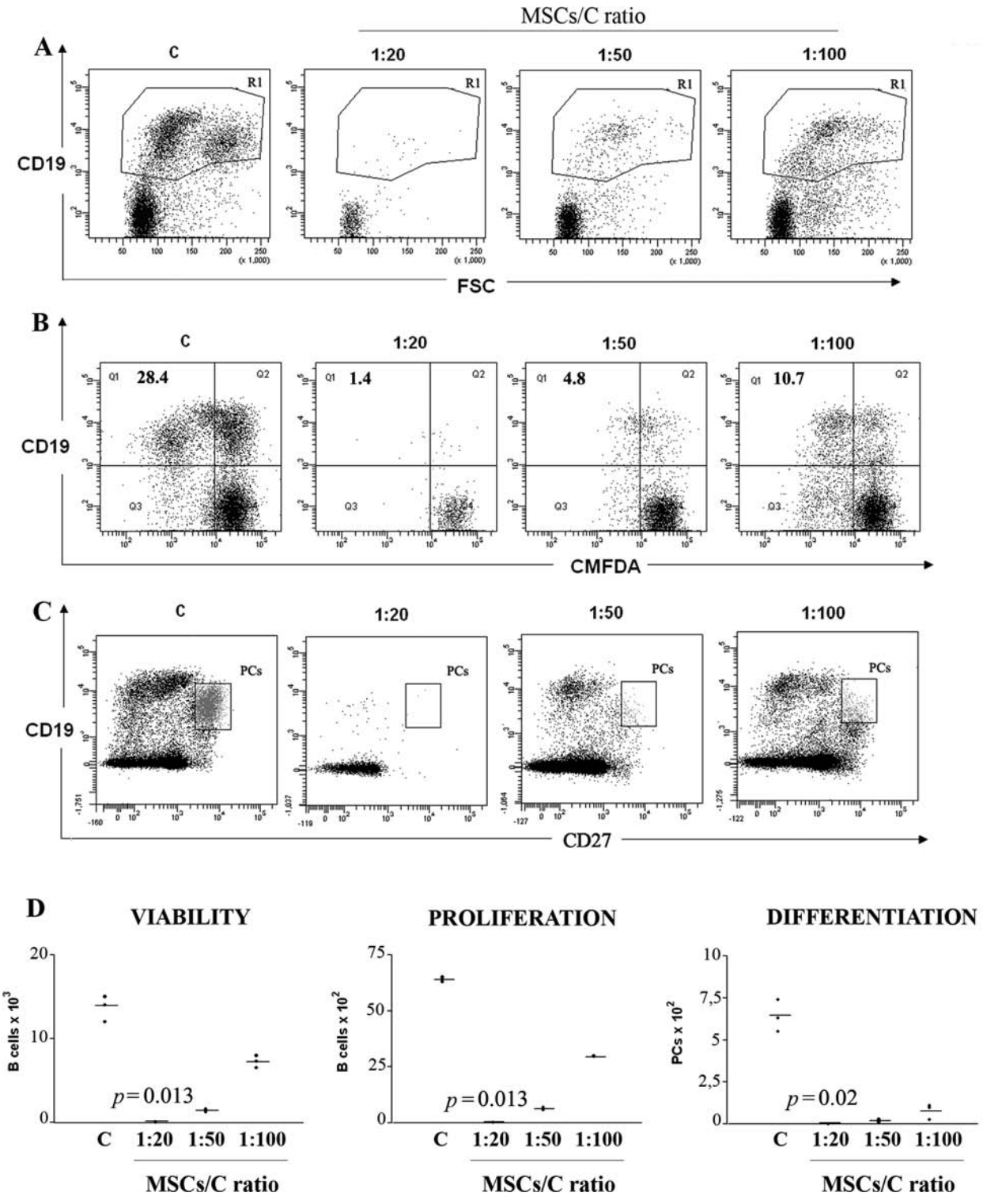

Figure 1. Coculture of CpG-stimulated PBMCs with MSCs. (A–C) Representative density plots. Cytometric analysis was performed by morphological parameter (forward scatter, FSC-H) of chloromethylfluorescein diacetate (CMFDA)-labeled peripheral blood mononuclear cells (PBMCs) (C) or PBMCs after coculture with mesenchymal stromal cells (MSCs) (MSCs/C) at ratios of 1:20, 1:50, and 1:100, respectively. (A) Positive CD19 cells were gated in R1 from PBMCs cultured with or (C) without MSCs. (B) In the top left quadrant (Q1), the percentage of CD19/CMFDA-positive cells is shown for PBMCs cultured with or (C) without MSCs. (C) Double-positive CD19/CD27 Plasma cells (PCs) are shown for PBMCs cultured with or (C) without MSCs. (D) Inhibition of viability, proliferation, and differentiation of CpG-stimulated B-cells in PBMCs cultured with or (C) without MSCs. Graphs show individual data and medians of three independent experiments.

nonparametric analysis of variance (Kruskal–Wallis test) followed by multiple comparisons by mean ranks was performed to compare quantitative data among groups. Linear regression analysis was performed to evaluate dose–response relationships. A value of $p < 0.05$ was considered statistically significant.

RESULTS

Coculture of PBMCs With MSCs

We first investigated the effects of MSCs on B-cell viability upon stimulation with CpG. We cocultured CMFDA-labeled PBMCs (C) isolated from $n = 8$ healthy donors with MSCs. After 7 days of incubation, we analyzed the CD19-positive cells by cytometric analysis. A significant inhibition of B-cell viability was observed at the MSC/C ratio of 1:20 (Fig. 1A, D). We next investigated whether coculture with MSCs affects B-cell proliferation and differentiation. After 7 days in the previously described experimental conditions, double-stained CD19/CMFDA and CD19/CD27 cells were gated in flow cytometry analysis. Maximum inhibition of B-cell proliferation (Fig. 1B, D) and differentiation (Fig. 1C, D) was observed at 1:20 MSCs/C ratio.

Effect of MSC-MVs on B-Cell Proliferation and Differentiation

MSC-MVs were added to PBMCs at 1 and 24 h after seeding. Statistically significant inhibition of B-cell proliferation was observed in the presence of MSC-MVs (Fig. 2A, top; B). The differentiation of plasma cells (PCs) from B lymphocytes was also evaluated by double staining with CD19 and CD27. A strong inhibition of PCs

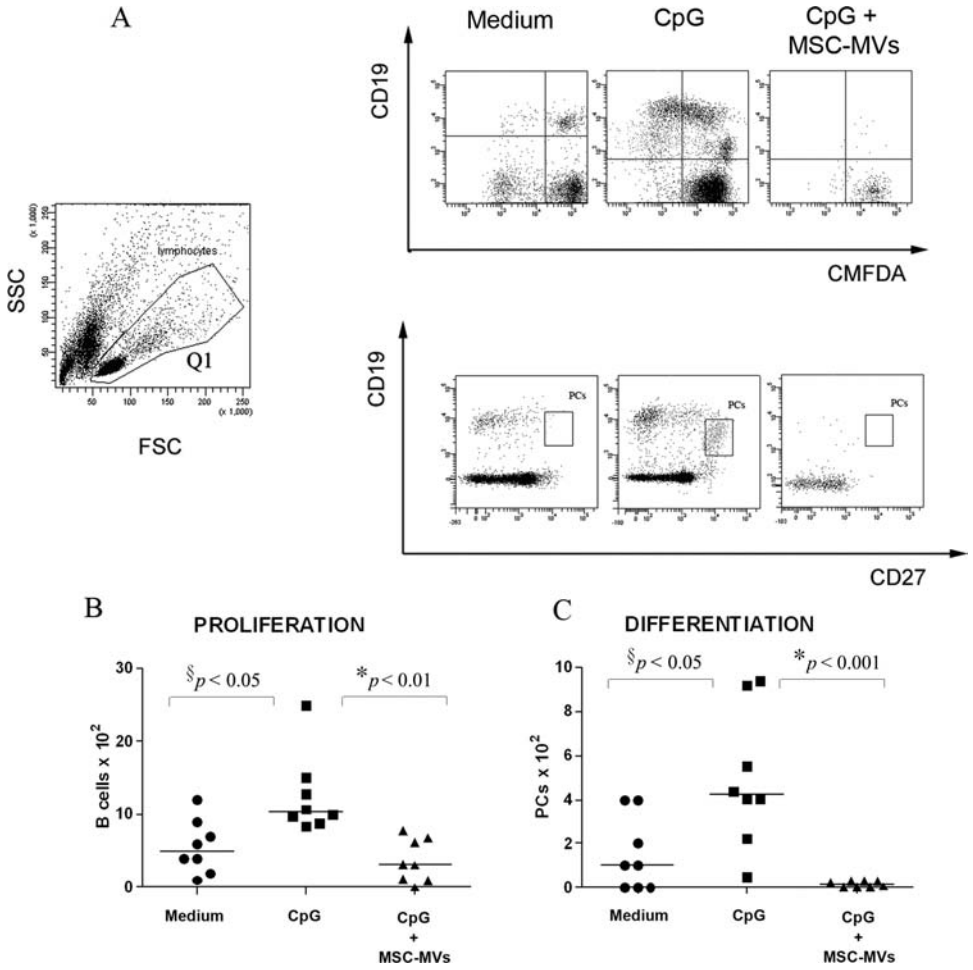

Figure 2. Effect of MSC-MVs on CpG-stimulated PBMCs. (A) Representative density plots of cytometric analysis of CMFDA-labeled PBMCs cultured in medium alone, with CpG, or with MSC-membrane vesicles (MVs) and CpG. Lymphocytes were gated in Q1 by morphological parameters (FSC-H; SSC-H) as living cells (left). They were subsequently analyzed either for the proliferation rates by CMFDA/CD19 staining (top right) or for the differentiation stage of plasma cells (PCs) by selecting CD19/CD27-positive events (bottom right). (B) Inhibition of proliferation of CMFDA/CD19-positive lymphocytes from a culture of PBMCs cultured in medium alone, with CpG, or with MSC-MVs and CpG. (C) Inhibition of differentiation of CD19/CD27-positive plasma cells (PCs) from a culture of PBMCs cultured in medium alone, with CpG, or with MSC-MVs and CpG. Graphs show individual data and medians of four independent experiments.

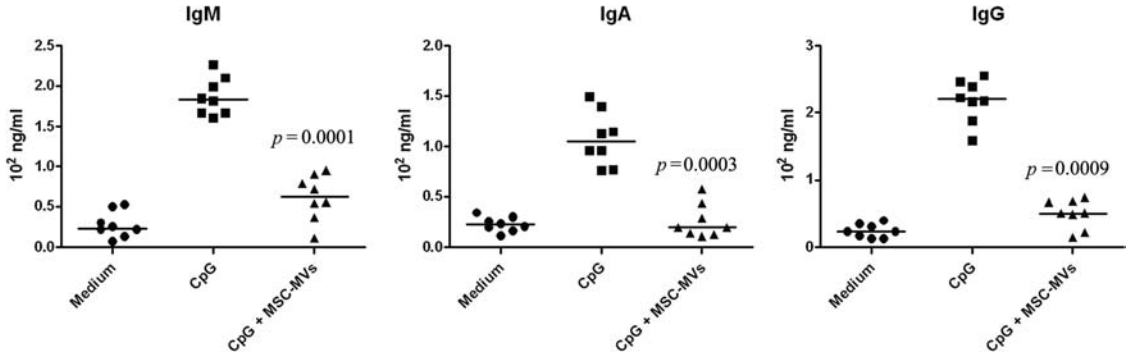

Figure 3. Inhibition of immunoglobulin production in CpG-stimulated PBMCs after incubation with MSC-MVs. ELISA assay of supernatants from a culture of PBMCs cultured in medium alone, with CpG, or with MSC-MVs and CpG. Graphs show individual data and medians of IgM, IgG, or IgA concentrations (10^2 ng/ml) in four independent experiments.

was observed in the presence of MSC-MVs (Fig. 2A, bottom; C). MSC-MVs also inhibited the production of IgM, IgG, and IgA by PBMCs (Fig. 3).

Apoptosis

The percentage of Annexin V/7-AAD-positive B lymphocytes (approximately 2% of the total B lymphocytes) was not statistically different among cells cultured with medium alone, with CpG alone, or with CpG and MSC-MVs both after 4 days and after 7 days in culture, indicating that the suppressive effect of MSC-MVs was not associated with B-cell death. For the sake of simplicity, only data at day 7 are shown (Fig. 4).

Characterization of MSC-MVs

A representative density plot of the MSC-MVs population isolated as described above is shown in Figure 5. MSC-MVs are 7-AAD-negative and express Annexin V.

Dose-Dependent Effect of MSC-MVs on B Lymphocytes

Serial dilutions of the MSC-MV suspension, obtained as described above, were added to 5×10^5 PBMC cultures. A linear correlation was found between MSC-MV concentration and the inhibiting effect on B lymphocytes, with respect to both cell proliferation and differentiation (Fig. 6A). A dose-dependent inhibitory effect of MSC-MVs was also observed on IgM, IgG, and IgA production (Fig. 6B).

Cytokine Content of MSC-MVs

Both IL-6 and IL-8 were detectable in MSC-MV lysate and were released in culture medium. Both lysate and culture medium tested negative for IFN-γ, IL-1β, IL-2, IL-4, IL-5, IL-10, IL-12 p70, TNF-α, and TNF-β.

Analysis of MSC-MV Association With PBMCs

Flow cytometry analysis of PBMCs preincubated with PKH26-labeled MSC-MVs revealed that these particles were associated with a subset of CD86/CD19-positive cells corresponding to B lymphocytes. No association of labeled MSC-MVs was found either with CD3-positive cells (corresponding to T lymphocytes) or with CD56-positive cells (corresponding to natural killer cells) (Fig. 7).

In order to further evaluate the association of MSC-MVs with specific cell phenotypes, we performed an immunofluorescence analysis of PBMC samples preincubated or not with labeled MSC-MVs by confocal laser scanning microscopy (Fig. 8). A panel of fluorescently labeled antibodies directed to CD3, CD19, CD56, and CD86 molecules was used, and the colocalization analysis revealed a consistent association of MSC-MVs with CD19- and CD86-positive cells, whereas no association was observed with CD3- and CD56-positive cells (Fig. 9). The analysis of the localization of red fluorescently labeled MSC-MVs within cells was based on the Z-reconstruction of serial single optical sections of

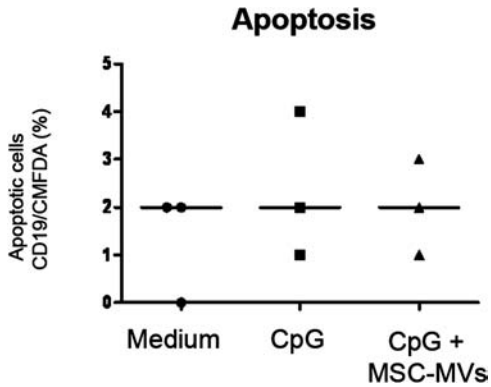

Figure 4. Detection of apoptosis. Annexin V/7-amino-actinomycin (7-AAD) analysis of proliferating CD19-positive cells maintained for 7 days in medium alone, with CpG, or treated with MSC-MVs plus CpG. Graphs show individual data and medians of three independent experiments.

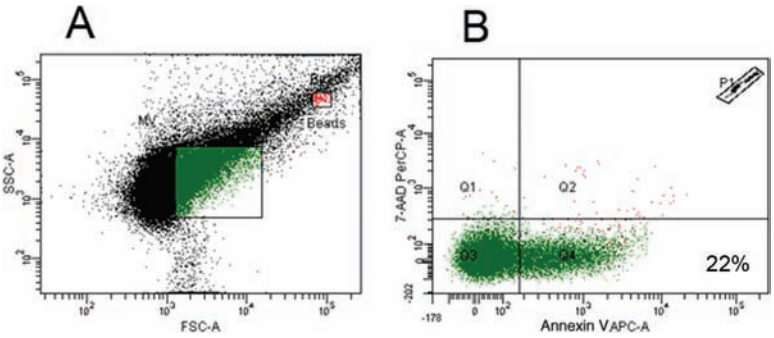

Figure 5. Flow cytometry analysis of MSC-MVs. Representative scatter plot obtained by flow cytometry of MSC-MVs. (A) The MSC-MVs were gated using size calibration beads to define the proper gate of events within 0.5- to 1-μm dimensions. (B) MSC-MVs derived from the gate shown in (A) were identified in quadrant Q4 by Trucount beads (P1), Annexin V positivity, and 7-AAD negativity. The percentage of Annexin V-positive/7-AAD-negative MSC-MVs is indicated in Q4.

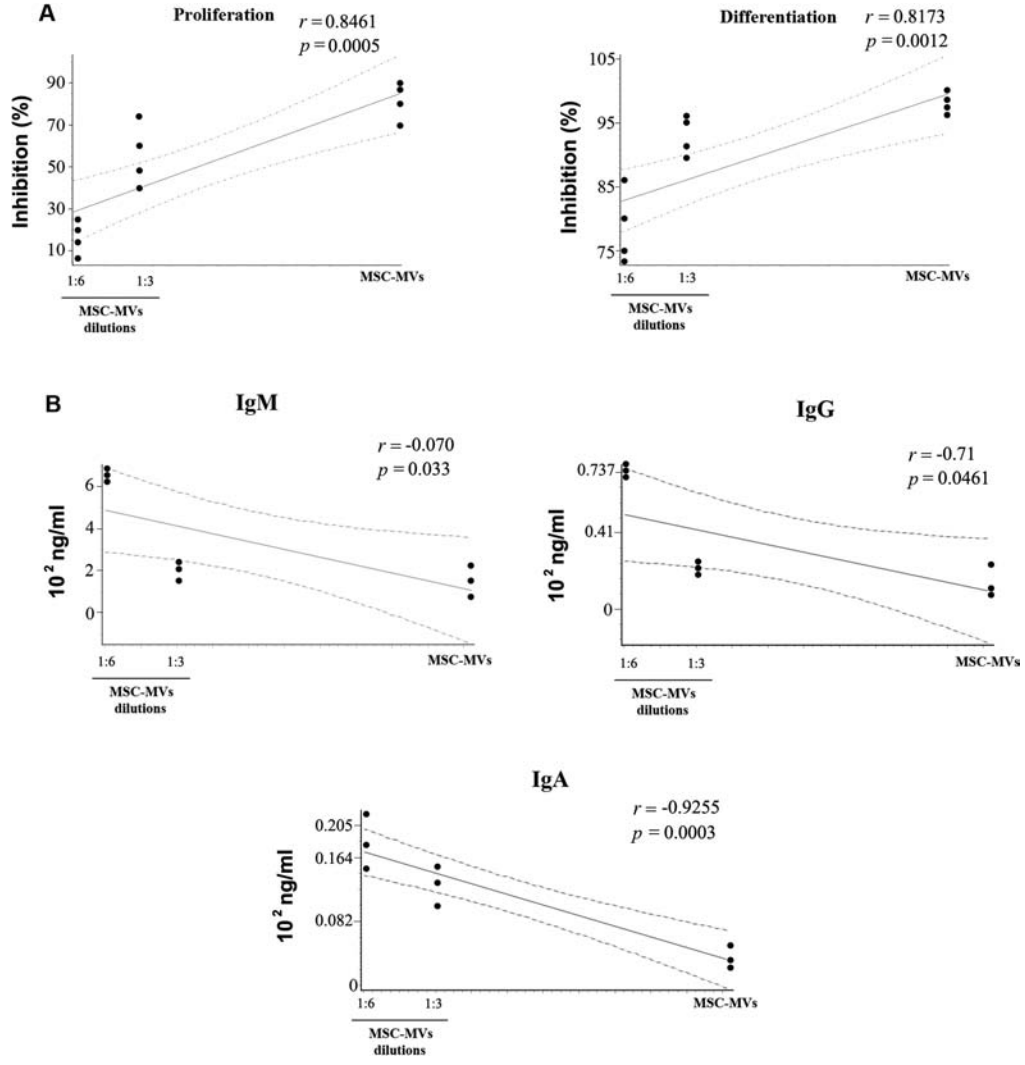

Figure 6. Dose-dependent inhibitory effect of MSC-MVs on B lymphocytes. (A) Inhibition of proliferation (left) and differentiation (right) of CpG-stimulated PBMCs after culture with undiluted MSC-MVs and at 1:3–1:6 dilutions. (B) Immunoglobulin ELISA assay of supernatants from a culture of PBMCs alone (not shown) or incubated with MSC-MVs at 1:3 or 1:6 dilutions. A significant dose-dependent inhibition of IgM, IgG, and IgA production was observed. The results were obtained from four independent experiments.

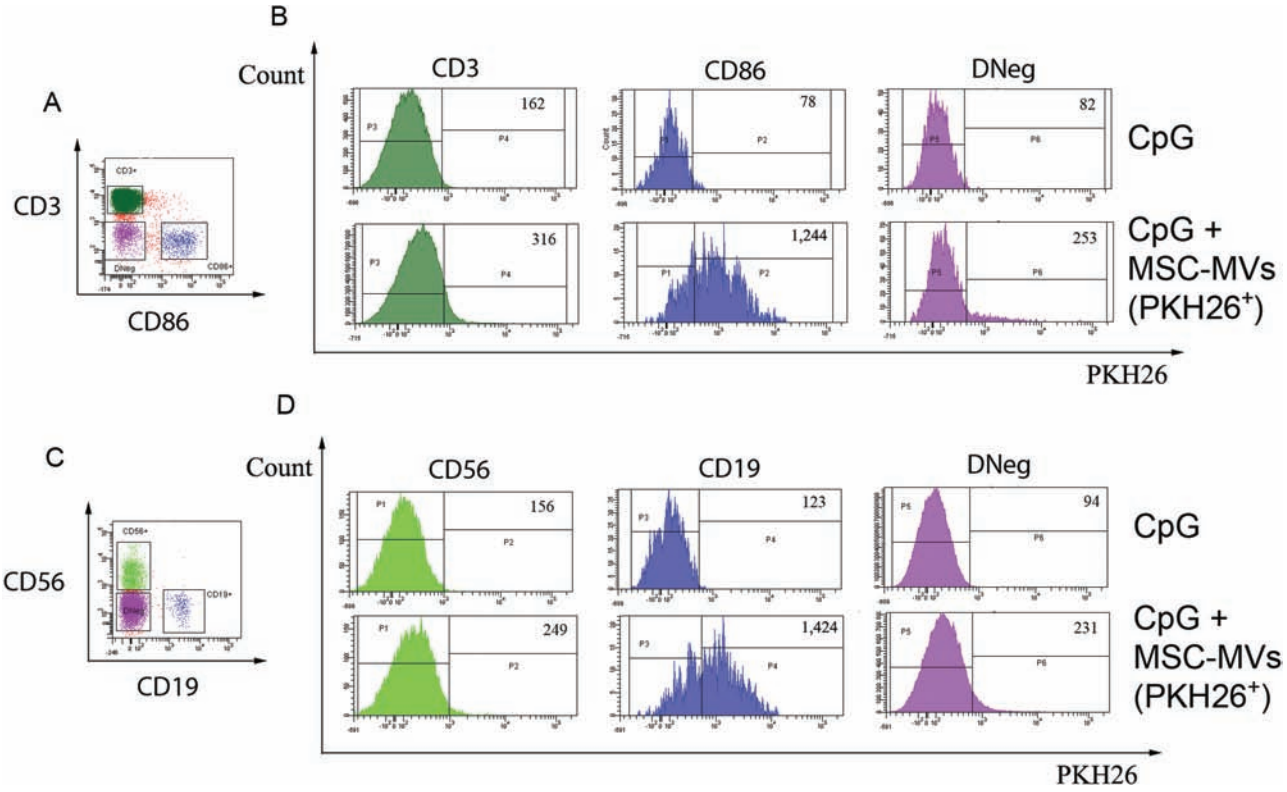

Figure 7. Fluorescence-activated cell sorting (FACS) analysis of the association between PKH26-labeled MSC-MVs and selected cell phenotypes in CpG-stimulated PBMCs. (A) Density plots of $CD3^+$, $CD86^+$, and double-negative lymphocytes (DNeg), selected in three different gates. (B) Histograms of fluorescence intensity (IF) of CD3-FITC-, CD86-APC-positive gated lymphocytes analyzed before (top) or after incubation with PKH26-labeled MSC-MVs (bottom). (C) Density plots of $CD56^+$, $CD19^+$, and double-negative lymphocytes (DNeg), selected in three different gates. (D) Histograms of IF of CD56-FITC-, CD19-APC-Cy7-positive gated lymphocytes analyzed before (top) or after incubation with PKH26-labeled MSC-MVs (bottom). After incubation with PKH26-labeled MSC-MVs, the levels of IF (plotted values in the top right quadrant) increased in $CD86^+$ cells (IF = 1,244 vs. basal level IF = 78) and $CD19^+$ cells (IF = 1,424 vs. basal level IF = 123).

CD19- and CD86-positive cells (Fig. 9). The MSC-MV distribution in the lateral and axial dimensions, visualized by *xz*- and *yz*-axis projections, confirmed their intracellular localization in the cytoplasm of CD19- and CD86-positive cells (Fig. 9).

DISCUSSION

The immunomodulatory effect of MSCs on B-cells is still controversial, and the mechanisms involved are unclear (8,10,22,26,28,30). Because of the documented species differences (23), we will discuss previously published work with human cells only. The role of soluble factors is generally recognized, and it was found to be more relevant in mediating the effect on B than on T lymphocytes (1). It has been proposed that the conflicting results between different laboratories could derive from differences in the methods used to isolate and characterize MSCs (21). For our studies, we relied on a commercial MSC preparation, which in our hands demonstrated good batch-to-batch reproducibility in the present experimental setup (data not shown). Also, we studied the effect of MSCs in culture with PBMCs rather than with purified B-cells, since the former is a more physiological system, including all immune-competent cells.

We observed that MSCs exert a strong inhibitory effect on B-cell proliferation and differentiation in PBMCs, in agreement with previous reports (8,10,26) but not with others (22,28). Both effects could be fully reproduced with MSC-MVs. MSC-MVs affected also B-cell lineage function, as shown by the strong inhibition on immunoglobulin secretion. Also, a linear relationship was observed between MSC-MV concentration and inhibition of B-cell proliferation and differentiation.

It has been reported that the suppressive effect of MSCs on B-cells was still present when separating PBMCs and MSCs by a permeable membrane (1,10). However, such inhibition was absent (10) or only partial (1) when using MSC supernatant. It was thus hypothesized that the inhibitory effect of MSCs required

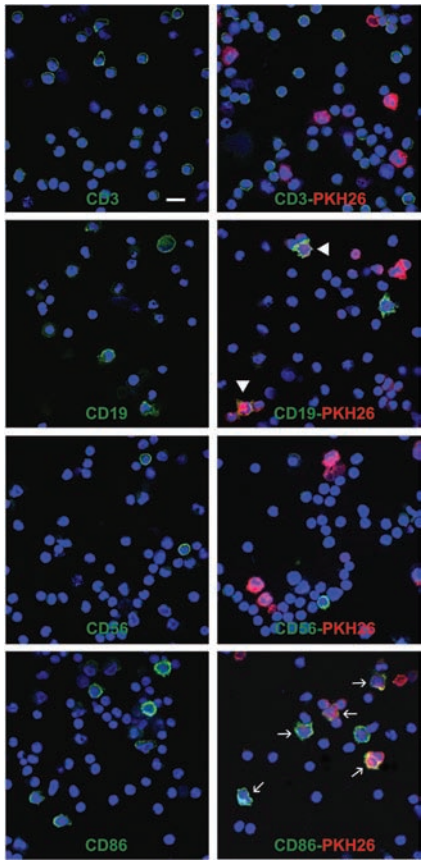

Figure 8. Confocal microscopy of the association between PKH26-labeled MSC-MVs and selected cell phenotypes in CpG-stimulated PBMCs. PBMCs immunolabeled with antibodies against CD3, CD19, and CD86 conjugated to allophycocyanin (pseudocolored in green) and FITC-conjugated CD56 (green), with (right) and without (left) incubation with PKH26-labeled MVs (red). Nuclei were counterstained with Hoechst. MSC-MVs were only associated with CD19-positive (arrowheads) and CD86-positive (arrows) cells. Scale bar: 10 μm.

cell-to-cell contact or the release of paracrine signals from B-cells in order to be fully expressed (10). However, the present results show that the MSC effect on both B-cell proliferation and differentiation can be fully reproduced by MSC-MVs in a dose-dependent fashion. We thus hypothesize that the concentration of MSC-MVs in the microenvironment surrounding B-cells could determine the degree of inhibition and could play a role as a regulatory factor in vivo, since MSCs migrate to inflammation sites (11). Experimental differences affecting MSC-MV availability to B-cells can probably explain previous conflicting results.

In order to evaluate whether other cell types present in PBMCs were involved in the observed phenomenon, we labeled MSC-MVs with a fluorescent dye and found them to be associated only with stimulated B-cells, both by FACS analysis and confocal microscopy.

These data suggest that the suppressive effect of MSCs on B-cells is largely mediated by MV release. The role of MVs as conveyors of immune response has been demonstrated in several pathways, involving all immune cell phenotypes (27). MVs derived by MSCs have been previously described as possible mediators of the antiapoptotic (13) and proregenerative effects (3,15) associated with MSC administration. However, their role in mediating MSC-induced B-cell suppression was not described so far. We found that MSC-MVs contain IL-6 and IL-8. IL-6 production by MSCs has been described previously (22). Clearly, the identification of these cytokines in MSC-MVs does not allow to draw any immediate hypothesis on the mechanisms underlying their immunosuppressive effect. Even if in our experimental setup these particles were found to be preferentially associated with stimulated B-cells, the observed effect could result from an interplay with other cell types present in PBMCs. In order to characterize the MSC-MVs preparations, we used Annexin V binding as a morphological/functional marker. It is known (14) that due to phospholipid asymmetry, some MVs express phosphatidylserine (PS) on the outer surface and thus bind Annexin V. In our experience, approximately 22% of MSC-MVs bound Annexin V, in agreement with the findings of Connor et al. (9). The biological significance, if any, of these different MV populations is presently unknown.

MSCs were reported to have both inhibitory (8,10,26) and stimulatory (22,28) effects on B-cell proliferation,

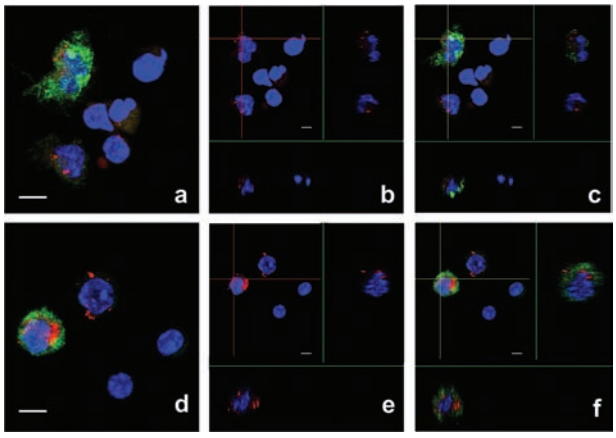

Figure 9. Confocal microscopy analysis of microphotographs of Z-reconstruction. The analysis of microphotographs of Z-reconstructions (a, d) performed by confocal laser scanning microscopy of CpG-stimulated PBMCs incubated with PKH26-positive MVs and stained with anti-CD19 (a–c) and anti-CD86 (d–f) antibodies. *xz*- and *yz*-axis projections (b–c, e–f) obtained from multiple consecutive optical sections, showing the intracellular localization of red fluorescently labeled MVs in CD19-positive (c, in green) and CD86-positive (f, in green) cells. Nuclei were stained with Hoechst. Scale bars: 5 μm (a, d) and 2 μm (b–c, e–f).

differentiation, and antibody production. Under some conditions, MSCs can function as antigen-presenting cells, thus enhancing the immune response (6). In one study involving interaction with B-cells, MSCs were found to exhibit opposite effects (i.e., either inhibitory or stimulatory), depending on the magnitude of the stimulus used to trigger the B-cells or on the different cell donors (22). Such unpredictable outcomes raise concern on the possibility to control the effect of administered MSCs in complex autoimmune disorders. MSC-MVs could possibly represent a safer and more reproducible therapeutic tool than MSCs. The clinical use of MVs was found to be both feasible and safe in phase I trials involving MVs derived from dendritic cells for immunotherapy of advanced cancer (12,20). Clearly, additional studies are needed to explore the role of MSC-MVs as modulators of immune response before they can be proposed for clinical use in place of the parent cells.

ACKNOWLEDGMENTS: This work was supported by the Italian Ministry of Health. We thank Paolo Parini for help with the statistical analysis and Rita Carsetti and Ezio Giorda for the FACS analysis. The authors declare no conflict of interest.

REFERENCES

1. Augello, A.; Tasso, R.; Negrini, S. M.; Amateis, A.; Indiveri, F.; Cancedda, R.; Pennesi, G. Bone marrow mesenchymal progenitor cells inhibit lymphocyte proliferation by activation of the programmed death 1 pathway. Eur. J. Immunol. 35:1482–1490; 2005.
2. Beyth, S.; Borovsky, Z.; Mevorach, D.; Liebergall, M.; Gazit, Z.; Aslan, H.; Galun, E.; Rachmilewitz, J. Human mesenchymal stem cells alter antigen-presenting cell maturation and induce T-cell unresponsiveness. Blood 105:2214–2219; 2005.
3. Bruno, S.; Grange, C.; Deregibus, M. C.; Saviozzi, S.; Collino, F.; Bussolati, B.; Tetta, C.; Camussi, G. Mesenchymal stem cell-derived microvesicles protect against acute tubular injury. J. Am. Soc. Nephrol. 20:1053–1067; 2009.
4. Caimi, P. F.; Reese, J.; Lee, Z.; Lazarus, H. M. Emerging therapeutic approaches for multipotent mesenchymal stromal cells. Curr. Opin. Haematol. 17:505–513; 2010.
5. Camussi, G.; Deregibus, M. C.; Bruno, S.; Cantaluppi, V.; Biancone, L. Exosomes/microvesicles as a mechanism of cell-to-cell communication. Kidney Int. 78:838–848; 2010.
6. Chan, J. L.; Tang, K. C.; Patel, A. P.; Bonilla, L. M.; Pierobon, N.; Ponzio, N. M.; Rameshwar, P. Antigen-presenting property of mesenchymal stem cells occurs during a narrow window at low levels of interferon-gamma. Blood 107:4817–4824; 2006.
7. Collino, F.; Deregibus, M. C.; Bruno, S.; Sterpone, L.; Aghemo, G.; Viltono, L.; Tetta, C.; Camussi, G. Microvesicles derived from adult human bone marrow and tissue specific mesenchymal stem cells shuttle selected pattern of microRNAs. PloS One 5:e11803; 2010.
8. Comoli, P.; Ginevri, F.; Maccario, R.; Avanzini, M. A.; Marconi, M.; Groff, A.; Cometa, A.; Cioni, M.; Porretti, L.; Barberi, W.; Frassoni, F.; Locatelli, F. Human mesenchymal stem cells inhibit antibody production induced in vitro by allostimulation. Nephrol. Dial. Transplant. 23:1196–1202; 2008.
9. Connor, D. E.; Exner, T.; Dang Fung Ma, D.; Joseph, J. E. The majority of circulating platelet-derived microparticles fail to bind Annexin V, lack phospholipid-dependent procoagulant activity and demonstrate greater expression of glycoprotein Ib. Thromb. Haemost. 103:1044–1052; 2010.
10. Corcione, A.; Benvenuto, F.; Ferretti, E.; Giunti, D.; Cappiello, V.; Cazzanti, F.; Risso, M.; Gualandi, F.; Mancardi, G. L.; Pistoia, V.; Uccelli, A. Human mesenchymal stem cells modulate B-cell functions. Blood 107:367–372; 2006.
11. da Silva Meirelles, L.; Caplan, A. I.; Nardi, N. B. In search of the in vivo identity of mesenchymal stem cells. Stem Cells 26:2287–2299; 2008.
12. Escudier, B.; Dorval, T.; Chaput, N.; André, F.; Caby, M. P.; Novault, S.; Flament, C.; Leboulaire, C.; Borg, C.; Amigorena, S.; Boccaccio, C.; Bonnerot, C.; Dhellin, O.; Movassagh, M.; Piperno, S.; Robert, C.; Serra, V.; Valente, N.; Le Pecq, J. B.; Spatz, A.; Lantz, O.; Tursz, T.; Angevin, E.; Zitvogel, L. Vaccination of metastatic melanoma patients with autologous dendritic cell (DC) derived exosomes: Results of the first phase I clinical trial. J. Transl. Med. 3:10–17; 2005.
13. Gatti, S.; Bruno, S.; Deregibus, M. C.; Sordi, A.; Cantaluppi, V.; Tetta, C.; Camussi, G. Microvesicles derived from human adult mesenchymal stem cells protect against ischaemia-reperfusion-induced acute and chronic kidney injury. Nephrol. Dial. Transplant. 26:1474–1483; 2011.
14. Gyorgy, B.; Szabò, T. G.; Pasztòi, M.; Pàl, Z.; Misjàk, P.; Aradi, B.; Làszlò, V.; Pàllinger, E.; Pap, E.; Kittel, A.; Nagy, G.; Falus, A.; Buzàs, E. I. Membrane vesicles, current state of the art: Emerging role of extracellular vesicles. Cell. Mol. Life Sci. 68:2667–2688; 2011.
15. Herrera, M. B.; Fonsato, V.; Gatti, S.; Deregibus, M. C.; Sordi, A.; Cantarella, D.; Calogero, R.; Bussolati, B.; Tetta, C.; Camussi, G. Human liver stem cell-derived microvesicles accelerate hepatic regeneration in hepatectomized rats. J. Cell. Mol. Med. 14:1605–1618; 2010.
16. Kebriaei, P.; Robinson, S. Treatment of graft-versus-host-disease with mesenchymal stromal cells. Cytotherapy 13:262–268; 2011.
17. Krampera, M.; Glennie, S.; Dyson, J.; Scott, D.; Simpson, E.; Dazzi, F. Bone marrow mesenchymal stem cells inhibit the response of naïve and memory antigen-specific T-cells to their cognate peptide. Blood 101:3722–3729; 2003.
18. Lamparski, H. G.; Metha-Damani, A.; Jenq-Yuan, Y.; Le Pecq, J. B. Production and characterization of clinical grade exosomes derived from dendritic cells. J. Immunol. Methods 270:211–226; 2002.
19. Meirelles Lda, S.; Fontes, A. M.; Covas, D. T.; Caplan, A. I. Mechanisms involved in the therapeutic properties of mesenchymal stem cells. Cytokine Growth Factor Rev. 20:419–427; 2009.
20. Morse, M. A.; Garst, J.; Osada, T.; Khan, S.; Hobeika, A.; Clay, T. M.; Valente, N.; Shreeniwas, R.; Sutton, M. A.; Delcayre, A.; Hsu, D. H.; Le Pecq, J. B.; Lyerly, H. K. A phase I study of dexosome immunotherapy in patients with advanced non-small cell lung cancer. J. Transl. Med. 3:9–17; 2005.
21. Ozaki, K.; Sato, K.; Oh, I.; Meguro, A.; Tatara, R.; Muroi, K.; Ozawa, K. Mechanisms of immunomodulation by mesenchymal stem cells. Int. J. Haematol. 86:5–7; 2007.
22. Rasmusson, I.; Le Blank, K.; Sundberg, B.; Ringdén, O. Mesenchymal stem cells stimulate antibody secretion in human B-cells. Scand. J. Immunol. 65:336–343; 2007.

23. Ren, G.; Su, J.; Zhang, L.; Zhao, X.; Ling, W.; L'huillie, A.; Zhang, J.; Lu, Y.; Roberts, A.I.; Ji, W.; Zhang, H.; Rabson, A. B.; Shi, Y. Species variation in the mechanisms of mesenchymal stem cell-mediated immunosuppression. Stem Cells 27:1954–1962; 2009.
24. Sattler, C.; Steinsdoerfer, M.; Offers, M.; Fischer, E.; Schierl, R.; Heseler, K.; Däubener, W.; Seissler, J. Inhibition of T-cell proliferation by murine multipotent mesenchymal stromal cells is mediated by CD39 expression and adenosine generation. Cell Transplant. 20:1221–1230; 2011.
25. Sheehy, M. E.; McDermott, A. B.; Furlan, S. N.; Klenerman, P.; Nixon, D. F. A novel technique for the fluorometric assessment of T lymphocyte antigen specific lysis. J. Immunol. Methods 249:99–110; 2001.
26. Tabera, S.; Perez-Simon, J.; Diez-Campelo, M.; Sanchez-Abarca, L. I.; Bianco, B.; Lopez, A.; Benito, A.; Ocio, E.; Sanchez-Guijo, F. M.; Canino, C.; San Miguel, J. F. The effect of mesenchymal stem cells on the viability, proliferation and differentiation of B-lymphocytes. Haematologica 93:1301–1309; 2008.
27. Théry, C.; Ostrowski, M.; Segura, E. Membrane vesicles as conveyors of immune responses. Nat. Rev. Immunol. 9:581–593; 2009.
28. Traggiai, E.; Volpi, S.; Schena, F.; Gattorno, M.; Ferlito, F.; Moretta, L.; Martini, A. Bone marrow-derived mesenchymal stem cells induce both polyclonal expansion and differentiation of B-cells isolated from healthy donors and systemic lupus erythematosus patients. Stem Cells 26:562–569; 2008.
29. Valadi, H.; Ekström, K.; Bossios, A.; Sjöstrand, M.; Lee, J. J.; Lötvall, J. O. Exosome-mediated transfer of mRNAs and microRNAs is a novel mechanism of genetic exchange between cells. Nat. Cell Biol. 9:654–669; 2007.
30. Yagi, H.; Soto-Gutierrez, A.; Parekkadan, B.; Kitagawa, Y.; Tompkins, R. G. ; Kobayashi, N.; Yarmush, M. L. Mesenchymal stem cells: Mechanisms of immunomodulation and homing. Cell Transplant. 19:667–679; 2010.
31. Zhao, S.; Wehner, R.; Bachmann, M.; Schimtz, M. Immunomodulatory properties of mesenchymal stromal cells and their therapeutic consequences for immune-mediated disorders. Stem Cells Dev. 19:607–614; 2010.